From Cosmology to Peaks in the Power Spectrum

Talk by Laura Sagunski,
Workshop Seminar on "The Planck Data", Summer Term 2013

April 30, 2013

Contents

1 Introduction and Review

The aim of this talk is to present how to calculate the power spectrum of CMB fluctuations analytically. To reveal the functional dependence of the power spectrum on the cosmological parameters, its main contributions will be additionally determined by numerical fits. If not marked otherwise, I will refer to the results presented in [2].

We will start with a review of the basic equations needed for the calculation of the power spectrum.

1.1 Correlation Function

The spectrum of CMB fluctuations is usually expressed in terms of correlation function

$$C(\theta) = \left\langle \frac{\delta T}{T_0}(\vec{n}_1)\, \frac{\delta T}{T_0}(\vec{n}_2) \right\rangle, \tag{1}$$

which describes the average of temperature fluctuations measured by photons coming from the directions $\vec{n}_1$ and $\vec{n}_2$, separated by an angle θ (where $\vec{n}_1 \cdot \vec{n}_2 = \cos(\theta)$).
The temperature fluctuations in the direction $\vec{n}$ at present conformal time η_o and location $\vec{x}_0$ are given by

$$\frac{\delta T}{T_0}(\eta_o, \vec{x}_o, \vec{n}) = \int \frac{d^3k}{(2\pi)^{\frac{3}{2}}} \left(\left(\Phi + \frac{\delta}{4} \right)_{\vec{k}} - \frac{3}{4} \frac{\delta'_{\vec{k}}}{k^2} \frac{\partial}{\partial \eta_0} \right)_{\eta_r} e^{i\vec{k}\cdot(\vec{x}_o + \vec{n}(\eta_r - \eta_o))}, \tag{2}$$

where Φ and δ correspond to the gravitational potential and the fluctuations of the photon energy density, while η_r refers to the moment of recombination. (The prime denotes the derivative with respect to conformal time.) In the above equation, the first term under the integral describes the combined result from the initial inhomogeneities in the radiation energy density and the Sachs-Wolfe effect, while the second term (the so-called Doppler contribution) is related to the velocities of the baryon-radiation plasma at recombination.

By inserting (2) in (1), the correlation function can be rewritten in the following form

$$C(\theta) = \frac{1}{4\pi} \sum_{l=2}^{\infty} (2l+1)\; C_l \, P_l(\cos(\theta)) \tag{3}$$

with

$$C_l = \frac{2}{\pi} \int k^2 dk \left| \left(\Phi_k(\eta_r) + \frac{\delta_k(\eta_r)}{4} \right) j_l(k\eta_0) - \frac{3}{4} \frac{\delta_k'(\eta_r)}{k} \frac{\partial j_l(k\eta_0)}{\partial \eta_0} \right|^2 \tag{4}$$

Thereby, the monopole and dipole components ($l = 0, 1$) were excluded. $P_l(\cos(\theta))$ and $j_l(k\eta)$ denote the Legendre polynomials and spherical Bessel functions, respectively.

1.2 Power Spectrum on Big Angular Scales

The formula (4) was derived in the approximation of instantaneous recombination. This approximation is suitable for big angular scales (corresponding to small multipole moments l) where the CMB fluctuations are mainly determined by inhomogeneities exceeding the horizon scale at recombination. On those super-horizon scales, the fluctuations in the photon energy density at recombination time η_r can be approximated as

$$\delta_k(\eta_r) \simeq -\frac{8}{3}\, \Phi_k, \quad \delta_k'(\eta_r) \simeq 0 \tag{5}$$

so that their contribution to the temperature fluctuations (cf. (2)) yields

$$\frac{\delta T}{T_0}(\eta_o, \vec{x}_o, \vec{n}) \simeq \frac{1}{3}\, \Phi(\eta_r, \vec{x}_0 - \eta_0\, \vec{n})\,. \tag{6}$$

Assuming a flat initial spectrum $\left(\left| \left(\Phi_k^0\right)^2 k^3 \right| = B \text{ with amplitude } B\right)$, substituting (5) in (4) and performing the integration, the power spectrum of CMB fluctuations for big angular scales arises as

$$(l\,(l+1)\; C_l)_{l<30} = \frac{9B}{100\pi} = \text{const.}, \tag{7}$$

constituting a good approximation for $l < 30$.

1.3 Delayed Recombination and Finite-Thickness Effect

On small angular scales, the process of recombination cannot be approximated as instantaneous effect anymore. Instead, the finite duration of recombination (delayed recombination) has to be taken into account. As a consequence the information about the place from where the photons arrive is "smeared out". This leads to a suppression of the CMB fluctuations in small angular scales, which is referred to as finite-thickness effect.

To account for the finite duration of recombination, the recombination moment η_r in the formula (2) should be replaced by the moment of last scattering η_L, weighted with the probability that the photon was scattered last time within the time interval $d\eta_L$,

$$dP(\eta_L) = \mu'(\eta_L)\, e^{-\mu(\eta_L)}\, d\eta_L \tag{8}$$

where $\mu\,(\eta_L)$ denotes optical depth and $\mu'(\eta_L)\, e^{-\mu(\eta_L)}$ equals the visibility function. The visibility function reaches its maximum in the "middle" of recombination at $z_r \simeq 1050$, irrespective of the values of the cosmological parameters.[1] Near its maximum it can be well approximated by the Gaussian function

$$\mu'(\eta_L)\, e^{-\mu(\eta_L)} \propto e^{-\frac{3}{2}\sigma^2 \left(\frac{\eta_L}{\eta_r}-1\right)^2}. \tag{9}$$

(The pre-exponential factor can be determined by normalization to unity.)

By substituting now (8) with (9) in (2) and estimating the gravitational potential Φ and the photon energy density δ at η_r to perform the integration over η_L, we obtain the modified expression

$$\frac{\delta T}{T_0} = \int \frac{d^3k}{(2\pi)^{\frac{3}{2}}} \left(\left(\Phi + \frac{\delta}{4}\right)_{\vec{k}} - \frac{3}{4}\frac{\delta_{\vec{k}}'}{k^2}\frac{\partial}{\partial\eta_0} \right)_{\eta_r} e^{i\,\vec{k}\cdot(\vec{x}_o + \vec{n}\,(\eta_r - \eta_o))}\; e^{-(\sigma\, k\eta_r)^2}. \tag{10}$$

Thus, in comparison to the case of instantaneous recombination, the key formula (2) has to be multiplied by a general factor $e^{-(\sigma\, k\eta_r)^2}$ under the integral to include the effect of delayed recombination (cf. (10)).

[1] In the following, we will refer to η_r as the maximum of the visibility function.

2 Power Spectrum on Small Angular Scales

The horizon scale at recombination corresponds to the multipole moment $l \simeq 200$. Hence, the perturbations, which are responsible for the fluctuations with $l > 100 \ldots 200$ in the power spectrum, entered the horizon before recombination. As they evolve in a rather complicated way, the spectrum of CMB fluctuations on small angular scales is (in distinction to the spectrum on big angular) strongly modified compared to the primordial spectrum and sensitively depends on the major cosmological parameters. At the moment of recombination η_r these fluctuations can be described by the following equations [2],

$$\Phi_k + \frac{\delta_k}{4} \simeq \left[T_p \left(1 - \frac{1}{3c_S^2}\right) + T_o \sqrt{c_S} \cos\left(k \int_0^{\eta_r} d\eta\, c_S(\eta)\right) e^{-\frac{k^2}{k_D^2}} \right] \Phi_k^0, \tag{11}$$

$$\delta_k' \simeq -4T_o k c_S^{\frac{3}{2}} \sin\left(k \int_0^{\eta_r} d\eta\, c_S(\eta)\right) e^{-\frac{k^2}{k_D^2}} \Phi_k^0, \tag{12}$$

wherein T_p and T_o denote the transfer functions relating the initial spectrum of gravitational potential Φ_k^0 to the resulting spectra for Φ and δ at η_r.
In the following, we will restrict our consideration to the (realistic) case $\Omega_b \ll \Omega_m$ where the baryon density Ω_b is much smaller than the total matter density Ω_m. This will in particular allow us to neglect the baryon contribution to the gravitational potential in the computation of the transfer functions.

2.1 Calculation of the Power Spectrum

2.1.1 Analytical Calculation of the Power Spectrum

Since we consider small angular scales, corresponding to big multipoles $l \gg 1$, the spherical Bessel functions $j_l(k\eta_0)$ in (4) (corrected by a factor $e^{-2(\sigma k\eta_r)^2}$ due to the finite-thickness effect) can be approximated analytically. The resulting expression was first derived in [5, 6, 7] and will be the starting point for our further calculations,

$$C_l \simeq \frac{1}{16\pi} \int_{\frac{l}{\eta_0}}^{\infty} dk \left(\frac{|4\Phi + \delta|^2 k^2}{k\eta_0 \sqrt{(k\eta_0)^2 - l^2}} + \frac{9\sqrt{(k\eta_0)^2 - l^2}}{(k\eta_0)^3} \delta_k'^2 \right) e^{-2(\sigma k\eta_r)^2}. \tag{13}$$

If we substitute the basic formulae (11) and (12) (assuming a flat initial spectrum $\left(\left|\left(\Phi_k^0\right)^2 k^3\right| = B\right)$) into the above equation for C_l and change the integration variable to $x \equiv \frac{k\eta_0}{l}$, the resulting expression for the power spectrum can be written as the sum of an oscillating contribution O and a non-oscillating contribution N,

$$l(l+1)\, C_l \simeq \frac{B}{\pi}\, (O + N). \tag{14}$$

Thereby, the oscillating contribution

$$O = O_1 + O_2 \tag{15}$$

which consists of two terms with twice different periods,

$$O_1 \equiv 2\sqrt{c_S}\left(1 - \frac{1}{3c_S^2}\right) \int_1^{\infty} dx\, \frac{T_p(x)\, T_o(x)\, e^{-\frac{l^2x^2}{2}\left(\frac{1}{l_S^2} - \frac{1}{l_f^2}\right)^2}}{x^2\sqrt{x^2-1}} \cos(l\varrho x)\,, \tag{16}$$

$$O_2 \equiv \frac{c_S}{2} \int_1^{\infty} dx\, \frac{T_o^2(x)\left[\left(1 - 9c_S^2\right)x^2 + 9c_S^2\right] e^{-\frac{l^2x^2}{l_S^2}}}{x^4\sqrt{x^2-1}} \cos(2l\varrho x)\,, \tag{17}$$

modulates the spectrum by generating its characteristic peaks and valleys. In particular, it depends on the parameter ϱ determining the period of oscillations and therefore the location of the peaks. Besides, the oscillating contributions are dependent on the speed of sound c_S, the damping scales l_f and l_S as well as on the transfer functions T_p and T_0. We will discuss these parameters and especially their relation to cosmology in detail in the following section (cf. 2.1.2).

Similarly, the non-oscillating contribution

$$N = N_1 + N_2 + N_3 \tag{18}$$

can be written as a sum of three integrals, namely

$$N_1 \equiv \left(1 - \frac{1}{3c_S^2}\right)^2 \int_1^\infty dx\, \frac{T_p^2(x)\; e^{-\frac{l^2 x^2}{l_f^2}}}{x^2\,\sqrt{x^2-1}}, \tag{19}$$

$$N_2 \equiv \frac{c_S}{2} \int_1^\infty dx\, \frac{T_o^2(x)\; e^{-\frac{l^2 x^2}{l_S^2}}}{x^2\,\sqrt{x^2-1}}, \tag{20}$$

$$N_3 \equiv \frac{9c_S^3}{2} \int_1^\infty dx\, \frac{T_o^2(x)\; e^{-\frac{l^2 x^2}{l_S^2}}\;\sqrt{x^2-1}}{x^4}. \tag{21}$$

Thereby, the contribution N_1 is proportional to the baryon density and vanishes in the absence of baryons when $c_S^2 = \frac{1}{3}$, as we will see from the definition of the speed of sound c_S in the following section.

2.1.2 Parameters Entering the Power Spectrum

Before we proceed further with the calculation of the integrals in (16)-(21), we will express the parameters entering the power spectrum (14), namely, c_S, l_f, l_S as well as T_o, T_p and ϱ, in terms of the basic cosmological parameters Ω_b, Ω_m and $\Omega_\Lambda = 1 - \Omega_m$ (for a flat universe).

Speed of sound $c_S(\Omega_b)$. To characterize how the speed of sound c_S at recombination deviates from the speed of sound in an ultrarelativistic medium, one introduces the parameter ξ is by

$$c_s^2 = \frac{1}{3\,(1+\xi)} \tag{22}$$

with

$$\xi(\Omega_b) \equiv \frac{1}{3c_S^2} - 1 = \frac{3}{4}\left(\frac{\varepsilon_b}{\varepsilon_\gamma}\right)_r \simeq 17\,\Omega_b h_{75}^2. \tag{23}$$

(In the numerically fitted last expression of (23), h_{75} denotes the Hubble parameter normalized to 75 $\frac{km/s}{\mathrm{Mpc}}$.) Thus, the speed of sound c_S at recombination depends only on the baryon density Ω_b. In the absence of baryons, $\Omega_b h_{75}^2 = 0$ so that $\xi = 0$, it equals $c_S^2 = \frac{1}{3}$ (ultrarelativistic medium), while for a realistic value of baryon density $\Omega_b h_{75}^2 \simeq 0.035$ where $\xi \simeq 0.6$ it yields $c_S^2 \simeq 0.2$ ($\Rightarrow c_S \simeq 0.46$).

Damping scales $l_f(\Omega_m)$ and $l_S(\Omega_b, \Omega_m)$. The scales l_f and l_S, which characterize the damping of the CMB fluctuations due to the finite-thickness effect and the so-called Silk dissipation[2], arise from (14) as

$$\frac{1}{l_f^2} \equiv 2\sigma^2\left(\frac{\eta_r}{\eta_0}\right)^2, \tag{24}$$

$$\frac{1}{l_S^2} \equiv 2\left(\sigma^2 + \frac{1}{k_D\eta_r}\right)\left(\frac{\eta_r}{\eta_0}\right)^2 \tag{25}$$

with

$$\sigma \simeq 1.49\cdot 10^{-2}\left(1 + \frac{1}{\sqrt{1+\frac{z_{eq}}{z_r}}}\right). \tag{26}$$

The exact value of z_{eq} depends on the contribution of the matter density to the total energy density and on the number of the ultrarelativistic species. Assuming three types of neutrinos, the ratio $\frac{z_{eq}}{z_r}$ can be estimated as

$$\frac{z_{eq}}{z_r} \simeq 12.8\,\Omega_m h_{75}^2 \tag{27}$$

where $z_r \simeq 1050$ (cf. 1.3).
To express the scales l_f and l_S in dependence on the cosmological parameters, we have to determine the Silk damping scale $(k_D\eta)_r$ and the ratio $\frac{\eta_r}{\eta_0}$. At recombination the Silk damping scale reads [2]

$$\frac{1}{(k_D\eta)_r^2} \simeq 0.36\,\frac{\sqrt{\Omega_m h_{75}^2}}{\Omega_b h_{75}^2}\,\frac{1}{z_r^{\frac{3}{2}}} + \frac{12}{5}\,c_s^2\sigma^2, \tag{28}$$

[2] resulting from the finite viscosity of the radiation-baryon plasma before recombination

wherein the first term, accounting for the dissipation until the beginning of recombination, is the same as in the case of instantaneous recombination, while the second term describes an extra contribution of Silk dissipation due to the delayed recombination.
The ratio $\frac{\eta_r}{\eta_0}$ is given by

$$\frac{\eta_r}{\eta_0} = \frac{1}{\sqrt{z_r}} \left(\sqrt{1 + \frac{z_r}{z_{eq}}} - \sqrt{\frac{z_r}{z_{eq}}} \right) I_\Lambda, \tag{29}$$

where the integral $I_\Lambda \simeq \Omega_m^{-0.09}$ is determined numerically by assuming a flat universe with $\Omega_\Lambda = 1 - \Omega_m$. After inserting the expressions for σ, $(k_D\eta)_r$ and $\frac{\eta_r}{\eta_0}$ in (24) and (25), we obtain for the damping scales l_f and l_S the following results,

$$l_f(\Omega_m) \simeq 1530 \sqrt{1 + \frac{z_r}{z_{eq}}} \frac{1}{I_\Lambda}, \tag{30}$$

$$l_S(\Omega_b, \Omega_m) \simeq 0.7 \frac{1}{\sqrt{\frac{1+0.56\xi}{1+\xi} + \frac{0.8}{\xi(1+\xi)} \frac{\sqrt{\Omega_m h_{75}^2}}{\left(1+\frac{1}{\sqrt{1+z_{eq}/z_r}}\right)^2}}} l_f. \tag{31}$$

Note that the damping scale l_S (in contrast to l_f) depends not only on the matter density Ω_m, but also on the baryon density Ω_b (via the parameter ξ).

Parameter $\varrho(\Omega_b, \Omega_m)$. From the oscillating contributions O_1 and O_2 (cf. (16), (17)) to the power spectrum one can see that the parameter ϱ determines the period of oscillations and the location of the peaks. By using the numerical fit for $\frac{z_r}{z_{eq}}$, it can be expressed as

$$\begin{aligned} \varrho(\Omega_b,\Omega_m) &\simeq \ln\left(\frac{\sqrt{\left(1 + \frac{z_r}{z_{eq}}\right)\xi} + \sqrt{1+\xi}}{1 + \sqrt{\frac{z_r}{z_{eq}}\xi}} \right) \\ &\simeq 0.014 \left(\Omega_m h_{75}^{3.1}\right)^{0.16} \frac{1}{1 + 0.13\,\xi}. \end{aligned} \tag{32}$$

Note that the parameter ϱ and therefore the characteristics of the peaks in the power spectrum depend both on the baryon density Ω_b and the matter density Ω_m.

Transfer functions $T_p(\Omega_m)$ and $T_o(\Omega_m)$. The first few peaks in the power spectrum are generated by perturbations which entered the horizon in between the time of matter-radiation equality and recombination. In this intermediate range $\left(1 < k\eta_{eq} < 10\right)$, the transfer functions T_p and T_0, which generally depend on the wavenumber k and the equality time η_{eq}, can be calculated only numerically. By introducing the variable $x \equiv \frac{k\eta_o}{l}$ by

$$k\eta_{eq} = \frac{\eta_{eq}}{\eta_0}\, lx \simeq 0.72 \frac{I_\Lambda}{\sqrt{\Omega_m h_{75}^2}} \frac{l}{200}\, x \tag{33}$$

and assuming $\Omega_b \ll \Omega_m$, the transfer functions in the relevant range of $k\eta_{eq}$ can be approximated for $200 < l < 1000$ by [1, 2]

$$T_p(x) \simeq 0.74 - 0.25\,(P + \ln(x)), \tag{34}$$

$$T_o(x) \simeq 0.50 + 0.36\,(P + \ln(x)), \tag{35}$$

where

$$P(l, \Omega_m, h_{75}) \equiv \ln\left(\frac{I_\Lambda}{\sqrt{\Omega_m h_{75}^2}} \frac{l}{200} \right). \tag{36}$$

2.1.3 Numerical Determination of the Power Spectrum

The form of integrals contained in the oscillating functions O_1 and O_2, (16) and (17), allows to calculate them by using the analytical expression

$$\int_1^\infty \frac{f(x)\cos(l\varrho x)}{\sqrt{x^2 - 1}} \simeq \sqrt{\frac{\pi}{l\varrho}}\, f(1) \cos\left(l\varrho + \frac{\pi}{4}\right), \tag{37}$$

which has been approximated for big l. Consequently, the oscillating contribution arises as

$$O(\Omega_b,\Omega_m) = O_1 + O_2 \simeq \sqrt{\frac{\pi}{l\varrho}} \left(A_1 \cos\!\left(l\varrho + \frac{\pi}{4}\right) + A_2 \cos\!\left(2l\varrho + \frac{\pi}{4}\right)\right), \tag{38}$$

where the coefficients A_1 and A_2 are slowly varying functions of l. Using the fact that the transfer functions T_p and T_o can be approximated in the range $200 < l < 1000$ (relevant for the first peaks) by the numerical fits (34) and (35), the coefficients A_1 and A_2 read

$$A_1(\Omega_b) \equiv -\left(\frac{4}{3\,(1+\xi)}\right)^{\frac{1}{4}} \xi\left(T_p T_o\right)_{x=1} e^{\frac{l^2}{2}\left(\frac{1}{l_S^2}-\frac{1}{l_f^2}\right)} \tag{39}$$

$$\simeq 0.1\, \frac{\left((P-0.78)^2 - 4.3\right)\xi}{(1+\xi)^{\frac{1}{4}}}\, e^{\frac{l^2}{2}\left(\frac{1}{l_S^2}-\frac{1}{l_f^2}\right)}, \tag{40}$$

$$A_2(\Omega_b) \equiv \frac{\left(T_o^2\right)_{x=1}}{4\sqrt{3\,(1+\xi)}} \tag{41}$$

$$\simeq 0.14\, \frac{(0.5 + 0.36\, P)^2}{\sqrt{1+\xi}}. \tag{42}$$

Analogously, the numerical approximations (34) and (35) of the transfer functions can be substituted in the non-oscillating contribution N_1 in (19). By defining subsequently the integrals

$$I_m\!\left(\frac{l}{l_f}\right) \equiv \int_1^\infty dx\, \frac{(\ln(x))^m}{x^2\sqrt{x^2-1}}\, e^{-\left(\frac{l}{l_f}\right)^2 x^2} \tag{43}$$

(which can be calculated analytically in terms of the hypergeometric functions) and fitting them numerically, we finally obtain the following result for the non-oscillating term N_1,

$$N_1(\Omega_b,\Omega_m) \simeq \xi^2\left[(0.74 - 0.25\,P)^2\; I_0 - (0.37 - 0.125\,P)\; I_1 + (0.25)^2\; I_2\right] \tag{44}$$

$$\simeq 0.063\,\xi^2\, \frac{\left(P - 0.22\left(\frac{l}{l_f}\right)^{0.3} - 2.6\right)^2}{1 + 0.65\left(\frac{l}{l_f}\right)^{1.4}}\, e^{-\left(\frac{l}{l_f}\right)^2}. \tag{45}$$

Similarly, the resulting expressions for the non-oscillating contributions N_2 and N_3, given by

$$N_2(\Omega_b,\Omega_m) \simeq 0.037\, \frac{1}{(1+\xi)^{\frac{1}{2}}}\, \frac{\left(P - 0.22\left(\frac{l}{l_f}\right)^{0.3} + 1.7\right)^2}{1 + 0.65\left(\frac{l}{l_f}\right)^{1.4}}\, e^{-\left(\frac{l}{l_f}\right)^2}, \tag{46}$$

$$N_3(\Omega_b,\Omega_m) \simeq 0.033\, \frac{1}{(1+\xi)^{\frac{3}{2}}}\, \frac{\left(P - 0.5\left(\frac{l}{l_f}\right)^{0.55} + 2.2\right)^2}{1 + 2\left(\frac{l}{l_f}\right)^{1.4}}\, e^{-\left(\frac{l}{l_f}\right)^2}, \tag{47}$$

can be deduced. Note that the numerical fits used in (45), (46) and (47) reproduce the exact results with an accuracy of a few percent within the relevant region $200 < l < 1000$ for a wide range of cosmological parameters.

The power spectrum for small angular scales of (14) is conveniently normalized to the corresponding spectrum for big angular scales, given by (7). Hence, we finally obtain the following result for the power spectrum of CMB fluctuations,

$$\frac{l\,(l+1)\; C_l}{(l\,(l+1)\; C_l)_{l<30}} = \frac{100}{9}\; (O + N_1 + N_2 + N_3)\,, \tag{48}$$

where the specific contributions O, N_1, N_2 and N_3 to the spectrum are given by (38), (45), (46) and (47), respectively.
The power spectrum based on (48) for the cosmological parameters $\Omega_m = 0.3$, $\Omega_\Lambda = 0.7$, $\Omega_b = 0.04$ and

$H = 70\,\frac{km/s}{\mathrm{Mpc}}$ is shown in Fig. 1. Thereby, the dashed and thin solid lines correspond to the non-oscillating and oscillating contributions, $N = N_1+N_2+N_3$ and O, while the total resulting spectrum of CMB fluctuations is represented by the thick solid line. The power spectrum (48) reproduces the numerical results with a good accuracy for a wide range of cosmological parameters. Only for very high values of the baryon density Ω_b and the matter density Ω_m, significantly deviations from the numerics arise. Furthermore, the peaks in the power spectrum are slightly shifted in comparison to the numerical results.

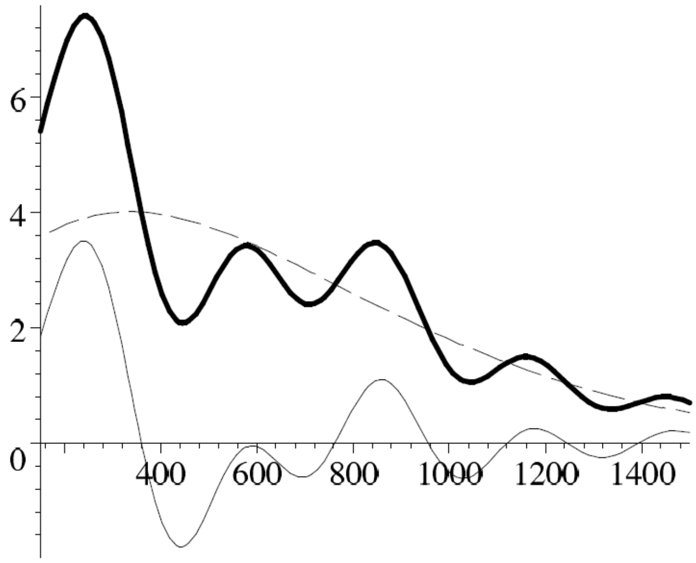

Figure 1: *Power spectrum of CMB fluctuations* $\frac{l(l+1)\,C_l}{(l(l+1)\,C_l)_{l<30}}$*, based on* (48)*, in dependence of the multipole moments* l *for the cosmological parameters* $\Omega_m = 0.3$*,* $\Omega_\Lambda = 0.7$*,* $\Omega_b = 0.04$ *and* $H_0 = 70\,\frac{km/s}{\mathrm{Mpc}}$. The total resulting power spectrum of CMB fluctuations (thick solid lines) can be separated into a non-oscillating contribution (dashed line) and an oscillating contribution (thin solid line).

2.2 Dependence of the Power Spectrum on the Cosmological Parameters

The power spectrum of CMB fluctuations depends in general on the cosmological parameters

$$\Omega_b,\ \Omega_m,\ h_{75},\ B \text{ and } n_S\,,$$

where B and n_s denote the amplitude and the spectral index of the primordial spectrum. (As before, the cosmological constant is fixed by the flatness condition to be $\Omega_\Lambda = 1-\Omega_m$). The peaks in the power spectrum constitute its most interesting feature since their location and height sensitively depends on these cosmological parameters. They arise as result of the superposition of the oscillating contribution O, given by (38), on the "hill" $N = N_1 + N_2 + N_3$ (cf. (45)-(47)) representing the non-oscillating part of the spectrum.

2.2.1 Location of the Peaks

If we consider only the oscillating contribution O in (38) and assume for the amplitudes $|A_1| \ll A_2$, the peaks should be located at

$$\cos\!\left(2l_n\varrho + \frac{\pi}{4}\right) \stackrel{!}{=} 1 \quad \Rightarrow l_n = \pi\left(n - \frac{1}{8}\right)\frac{1}{\varrho} \tag{49}$$

with $n \in \mathbb{N}$ and ϱ defined in (32). Since the first term in (38) has a twice bigger period than the second one as well as a negative amplitude (cf. (39)), the sum of these two terms results in constructive interference for the odd peaks ($n = 1, 3, \ldots$) and in destructive interference for the even peaks ($n = 2, 4, \ldots$). Due to the shift of the arguments of the two cosines, their maxima do not coincide so that the peaks should be located in between the maxima of the two cosines. Therefore, the location of the first peak should roughly at

$$l_1 \simeq \pi\left(\frac{6}{8}\ldots\frac{7}{8}\right)\frac{1}{\varrho}. \tag{50}$$

If $|A_1| \gg A_2$, the first peak moves closer to the lower bounds of the above interval. Besides, superimposing the non-oscillating contribution N leads to a further shift of the peak towards the "top of the hill".

Calculating the parameter ϱ of (32) for $\Omega_b h_{75}^2 \simeq 0.035$ ($\xi \simeq 0.6$) and $\Omega_m h_{75}^2 \simeq 0.26$ and using (50) afterwards, yields $l_1 \simeq 225 \ldots 265$ for the location of the first peak.

As the parameter $\varrho = \varrho(\Omega_b, \Omega_m)$ depends on the baryon and matter density, the location of the peaks (cf. (49)) consequently also depends on these parameters. In detail, an increase of the baryon density Ω_b leads to a shift of the peak locations to higher multipoles l (to the right in Fig. 1), whereas an increasing matter density Ω_m shifts the peaks in the opposite direction, i.e. to lower multipoles l (to the left). By simultaneously increasing the baryon and matter density, the location of the first peaks (for a fixed height) becomes stable. Hence, *the stability of the location of the first peak is a strong indicator for the total energy density of the universe.*[3]

2.2.2 Height of the Peaks

The height of the peaks, calculated by inserting the locations of the peaks l_n in the power spectrum (48), depends on the baryon and matter density as well.

Height of the first peak. While an increasing baryon density Ω_b raises the height of the first peak (mainly due to the contributions of $N_1 \propto \xi^2$ and O where $A_1 \propto \xi$), an increase in the matter density Ω_m leads to a decrease of the height of the first peak (mainly since the contributions N_2 and N_3 decrease when Ω_m increases). Therefore, in a certain range of parameters the increase of the height due to a higher baryon density can be compensated by simultaneously increasing the matter density. Since cosmology restricts Ω_m not to exceed unity too much (and the transfer functions, causing the dependence of the peak height on Ω_m, reach their asymptotic values in the region of the first peak), the *height of the first peak* allows us to *fix the relation between the baryon and matter density,* $\frac{\Omega_b}{\Omega_m}$. Moreover, we can conclude from the height of the first peak that *the baryon density can only constitute* $15 \ldots 20\,\%$ *of the total critical density*.

Height of the second peak. As the second peak results mostly from the destructive interference of the terms in the oscillating contribution O, its height sensitively depends on the ratio of the amplitudes A_1 and A_2. When enlarging the baryon density Ω_b, the negative amplitude A_1 of the first term increases and the second amplitude A_2 simultaneously decreases so that the second peak will be removed for high baryon densities. Hence the *presence of the second peak* can be considered as the indication of a *low baryon density being smaller than* $6 \ldots 8\%$ *of the matter density.*
Similarly, an increase of the matter density Ω_m, leading to a decrease of A_2 which is faster than the corresponding increase of A_1, tends to eliminate the second peak. By fixing the relation $\frac{\Omega_b}{\Omega_m}$ from the height of the first peak, *the height of the second peak requires the total matter density to be smaller than the critical one.* Thus, the height of the second peak sets a limit on the baryon density as well as on the matter density.

Height of the third peak. In the above calculations of the power spectrum we have assumed a flat universe with spectral index $n_S = 1$. However, inflation predicts a deviation of the spectral index from unity ($n_S \simeq 0.92 \ldots 0.97$ [3, 4]). For $n_s \neq 1$ the result for the power spectrum of (48) has to be modified by a factor $\propto l^{1-n_s}$.
Since the height of the third peak is more sensitive to the deviations of the spectral index than the heights (and locations) of the first two peaks, n_S is varied for a given unchanged height of the first peak (by simultaneously varying the amplitude B of the spectrum) whereby the relative height of the third peak changes as

$$\frac{\Delta H_3}{H_3} \propto \left(\frac{l_3}{l_1}\right)^{1-n_s} - 1. \tag{51}$$

Compared to the case $n_S = 1$, the height of the third peak increases by about 5% for $n_S \simeq 0.95$.

2.2.3 Dependence on the Hubble Parameter

Assuming a Hubble parameter higher than h_{75} shifts the location of the peaks to lower multipole moments l. However, for an accurate determination of the Hubble parameter from the power spectrum alone, the position of the peaks has to be determined with an extremely high accuracy (< 1% for an accuracy of 7% in the Hubble parameter).

[3] In an open universe without cosmological constant, the location of the first peak is even more sensitive to the total energy density since $l_1 \propto \frac{1}{\sqrt{\Omega_{tot}}}$.

References

[1] James M. Bardeen, J.R. Bond, Nick Kaiser, and A.S. Szalay. The Statistics of Peaks of Gaussian Random Fields. *Astrophys.J.*, 304:15–61, 1986.

[2] Viatcheslav F. Mukhanov. CMB-slow, or how to estimate cosmological parameters by hand. *Int.J.Theor.Phys.*, 43:623–668, 2004.

[3] Viatcheslav F. Mukhanov and G.V. Chibisov. Quantum Fluctuation and Nonsingular Universe. (In Russian). *JETP Lett.*, 33:532–535, 1981.

[4] Viatcheslav F. Mukhanov, H.A. Feldman, and Robert H. Brandenberger. Theory of cosmological perturbations. Part 1. Classical perturbations. Part 2. Quantum theory of perturbations. Part 3. Extensions. *Phys.Rept.*, 215:203–333, 1992.

[5] Steven Weinberg. Fluctuations in the cosmic microwave background. 1. Form-factors and their calculation in synchronous gauge. *Phys.Rev.*, D64:123511, 2001.

[6] Steven Weinberg. Fluctuations in the cosmic microwave background. 2. C(l) at large and small l. *Phys.Rev.*, D64:123512, 2001.

[7] Steven Weinberg. Cosmological fluctuations of short wavelength. *Astrophys.J.*, 581:810–816, 2002.